

# IDENTIFICATION OF HYDRO UNIT STIFFNESSES, CRITICAL SPEED AND VIBRATING MASSES BASED ON VIBRATION MEASUREMENTS

Ozren Husnjak  
Veski Ltd  
[ohusnjak@veski.hr](mailto:ohusnjak@veski.hr)

Ozren Oreskovic  
Veski Ltd  
[ooreskovic@veski.hr](mailto:ooreskovic@veski.hr)

John Letal  
Iris Power  
[jletal@qualitrolcorp.com](mailto:jletal@qualitrolcorp.com)

Fabian Kaica  
Fabian Kaica Consulting, Australia  
[fabiankaica@netspace.net.au](mailto:fabiankaica@netspace.net.au)

## SUMMARY

One of the most important procedures in evaluating the operational stability of a hydro unit is vibration measurement and analyses. The most important conclusion lies in the identification of permanent changes in the state as well as the determination of the type and location of changes. Any change in vibrational state can be related to the changes in the unit's construction properties (bearing, stator, bracket/foundation stiffnesses and vibrating masses of rotating/non-rotating construction elements). Identification of these properties shows that they are very often different for a real hydro unit when compared to the designed properties. A procedure was developed based on which a hydro unit's properties can be determined without the use of design data. In order to carry out the identification procedure it is necessary to conduct vibration measurements and analyses on all the bearings simultaneously. The results of the procedure are the oil film stiffness, stator stiffness, bracket/foundation stiffness, shaft stiffness and critical speeds.

As an example of the implementation of this procedure a reversible 180 MW hydro unit was used for which the bearing stiffnesses change significantly with thermal state (that is, stator and rotor thermal dilatations). Apart from the identification of the unit component's stiffnesses, a procedure for the first critical speed (cold and hot) was conducted. The results have shown that the calculated parameters from measured data compared to the design parameters are significantly different. For this reason there are significant vibrational problems in the operating regimes for which unexpected resonance states occur. The identification procedure can be performed with post processed data (stored waveform/trends data) originating from multi-channel measurement devices/analyzers and can also be embedded into the continuous on-line diagnostic monitoring systems for real time monitoring.

**Keywords:** critical speed, bearing/foundation stiffness, oil film stiffness, stator stiffness, shaft stiffness, experimental identification, real hydro unit parameters, vibrations

## INTRODUCTION

For most hydro-units the vibro-dynamical response of rotating and non-rotating parts is significantly dependent on the generator and turbine temperatures and, in particular, bearing temperatures. Significant changes in vibration levels (both relative and absolute vibrations) during temperature changes are observed even when the unit runs with unchanged active and reactive power. This kind of behaviour indicates there are significant changes in the stiffnesses of constructional elements and, consequently, its vibro-dynamical response. This is automatically reflected to the changes in the unit's critical speed which can significantly influence the unit's stability of operation, especially in transient operating regimes, such as load rejection.

In the tender documentation for new (or refurbishment of old) units there is often present a request that the unit's first critical speed is, at least, 20 % higher than the rotational speed reached in theoretical runaway. The hydro-unit OEMs often prove that this condition is met by performing critical speed numerical calculations. In practice, to test whether or not this condition is met is practically never done because the

owner of the unit doesn't allow the rotation in theoretical runaway speed and is, usually, satisfied with load rejection from maximum load.

Measurements performed on a large number of hydro-units have indicated that the described condition for critical speed is almost never satisfied. Often it's practically impossible to satisfy this condition.

In order to identify real vibration-related parameters, which are often significantly different than those given by the documentation, an experimental and calculation procedure to identify the real bearing stiffnesses, as well as rotating and non-rotating vibrating masses was developed. This procedure enables the identification of the real critical speed. The experiment that must be performed to enable the identification only uses the vibration measurement results for a unit with variable rotational speed (frequency) such as slow run-up or free run-down.

As an example for the identification – the vibrational response analysis for a reversible pump-generator unit (180 MW) is given. The main motive for the identification was that the critical speed when the unit starts cold was below nominal rotational speed which rarely is the condition for a hydro unit. Additionally, the calculated critical speed was two times higher than the measured critical speed providing more reason to identify the real vibration-related parameters.

### EXPERIMENTAL IDENTIFICATION OF THE HYDRO-UNIT VIBRATIONAL PARAMETERS – THE PROCEDURE

The experimental procedure used to identify the vibration-related parameters depends on the number of vibration measurement sensors installed on the unit. To determine the stiffnesses of the unit construction elements (shaft, bearings, foundation) it is necessary to install the vibration measurement sensors on all positions between which there are elastic deformations of the construction elements. This is the only way one can determine the stiffnesses of those structural elements.

On hydro units – the relative<sup>1</sup> shaft vibration sensors are typically installed along with absolute<sup>2</sup> bearing housing vibration sensors. Air gap sensors are also installed quite often and, sometimes, foundation vibration sensors (behind bearing housing or generator stator) are installed too. All of these sensors can be used to identify the unit's vibration-related parameters.

The identification procedure and results are given for a reversible pump-generator unit 180 MW.

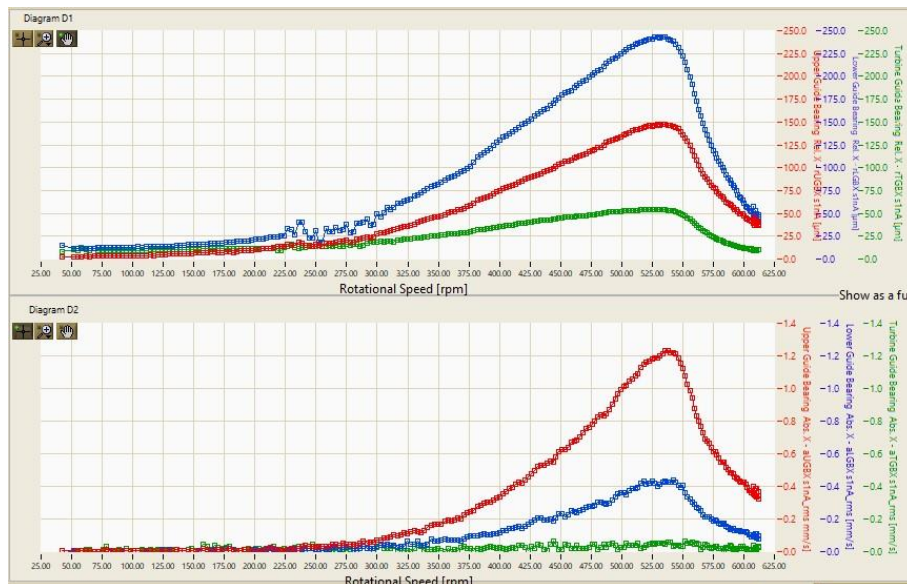


**Fig. 1 UPPER DIAGRAM: Relative shaft vibrations in one direction (X): UGB-X, LGB-X and TGB-X. LOWER DIAGRAM: Absolute bearing vibrations (vibrational velocity) in one direction (X): UGB-X, LGB-X and TGB-X. Both shown as a function of rotational speed.**

<sup>1</sup> relative means – shaft vibrations relative to the bearing housing

<sup>2</sup> absolute means – they measure the vibrations of the point they're attached to directly

For this unit, during the first rotating tests, the critical speed below the nominal rotational speed was observed. On Fig. 1 – relative and absolute vibrations (in the form of the 1x harmonic of rotational frequency) are given on all three bearings: UGB (Upper Guide Bearing), LGB (Lower Guide Bearing) and TGB (Turbine Guide Bearing) during the pump start from zero to 623 rpm. The unit’s nominal speed is ~600 rpm.

The diagrams show that the critical speed is on 540 rpm with large vibrations on LGB-X (240 µm peak). In the tender documentation – the calculated critical speed is given as 1150 rpm. Such a large difference between the calculated and real critical speed was the main reason to define the procedure for experimental identification of the vibration-related parameters in order to identify the main reason for such a large difference.

The diagrams on Fig. 1 show that the turbine rotor has a very small influence on the critical speed value. The small changes in relative vibrations are a consequence of the LGB vibrations which have reflected (with much smaller values) on a shaft near the turbine bearing. As seen from the absolute vibrations – there is almost a non-existent influence of the generator vibrations to the turbine bearing housing vibrational response near the first critical speed.

Such a relation is typical for a hydro-unit and the main conclusion is that only the generator masses and stiffnesses are relevant for the value of the first critical speed. This is an important assertion since the unit model can be simplified and the experimental identification procedures more easily defined. So, the identification procedure takes into account just the generator bearings.

The diagrams on Fig. 1 indicate non-linearity within the system. This can be seen by different slopes before and after passing through the critical speed. The non-linearity is present in the bearing oil film since it’s changing with vibration amplitudes, that is, with bearing clearance reduction. That’s why for the vibration-related parameters the parts of the curves on which the amplitudes are near maximum values were used.

Fig. 2 shows a model of the unit according to which the identification procedure is performed.

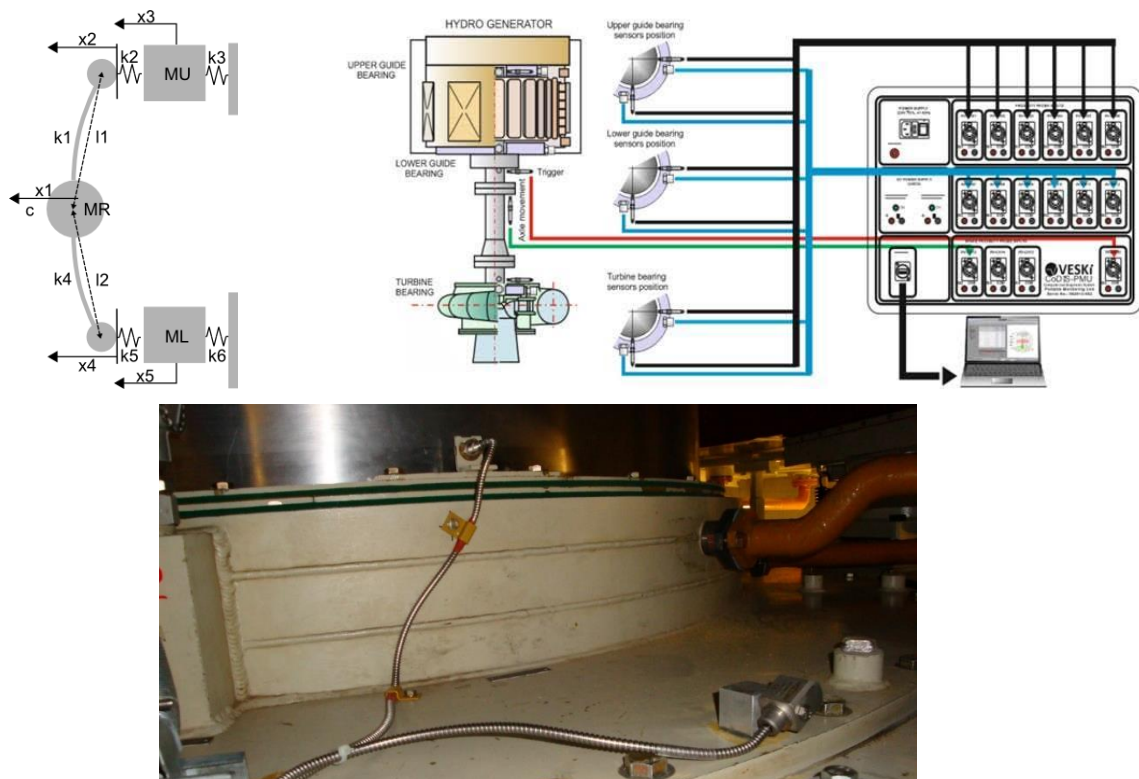


**Fig. 2 LEFT: Vibrational model with masses and stiffnesses indicated. RIGHT: Typical vibration measurement layout on a hydro unit. It can be used to detect the critical speed and stiffnesses. BOTTOM: Relative shaft and absolute bracket vibration sensors on LGB.**

This is the five (5) degrees of freedom system which is defined by the positions of the vibration measurement / analysis sensors. The basic displacement variables, as indicated by Fig. 2 are set to positions which are covered by the measurement sensors:

- $x_1$  are the rotor rim displacements (to determine these displacements, air gap sensors must be installed on a unit)
- $x_2$  and  $x_4$  are the (absolute) shaft displacements in the UGB and LGB zones (to determine these displacements both the relative shaft displacements (relative to the bearing housing) and absolute bearing housing displacements must be installed on a unit)
- $x_3$  and  $x_5$  are the UGB and LGB bearing housing displacements (to determine these displacements, absolute housing displacements must be installed on UGB and LGB)

The vibration-related parameters that are to be determined based on vibration measurements are:

- $M_R$ ,  $M_U$ ,  $M_L$  vibrating masses<sup>3</sup> ( $M_R$  = rotor vibrating mass,  $M_U$  = upper bracket with generator stator vibrating mass,  $M_L$  = lower bracket vibrating mass)
- $k_1$  and  $k_4$  are the stiffnesses of the upper and lower shaft parts
- $k_2$  and  $k_5$  are the stiffnesses of the UGB ( $k_2$ ) and LGB ( $k_5$ ) oil film
- $k_3$  and  $k_6$  are the stiffnesses of the upper bracket with generator stator ( $k_3$ ) and lower bracket ( $k_6$ )
- the damping characteristics of the system are attributed to the generator rotor with the coefficient  $C$  as a viscous damping element and the real damping coefficient will be determined based on vibrational response

From the displacement variables present in a model, the variables necessary for experimental identification are determined:

- $x_1$  = rotor absolute displacement
- $x_2-x_3$  = UGB relative displacements (relative vibrations)
- $x_4-x_5$  = LGB relative displacements (relative vibrations)
- $x_3$  = UGB absolute displacements (absolute vibrations)
- $x_5$  = LGB absolute displacements (absolute vibrations)

All of the displacements shown on Fig. 1 are the amplitudes (peak) of the first harmonic (rotational frequency harmonic). Generally, the displacement vectors are shown in the form  $X(\omega) = x(\omega) \exp(j\phi(\omega))$ . In the specific case (for this unit) all of the displacements are in phase (as seen from measurement results - ) for the rotational speed range so, only magnitudes are used in Eq. 1 and Eq. 2.

In order to perform the identification procedure – the expression (2) for the dynamical equilibrium between inertial and elastical forces on the positions of sensors:

$$\begin{aligned}
 -M_R \cdot \omega^2 \cdot x_1 + k_1 (x_1 - x_2) + k_4 (x_1 - x_4) + C \cdot j\omega \cdot x_1 &= F(\omega) \\
 k_1 (x_1 - x_2) \cdot l_1 &= k_4 (x_1 - x_4) \cdot l_2 \\
 k_1 (x_1 - x_2) - k_2 (x_2 - x_3) &= 0 \\
 k_4 (x_1 - x_4) - k_5 (x_4 - x_5) &= 0 \\
 -M_U \cdot \omega^2 \cdot x_3 - k_2 (x_2 - x_3) + k_3 x_3 &= 0 \\
 -M_L \cdot \omega^2 \cdot x_5 - k_5 (x_4 - x_5) + k_6 x_5 &= 0
 \end{aligned}$$

**Eq. 1 Equations of motion for a system shown on Fig. 2.**

If no air gap sensors are installed on a unit, the identification model is further simplified. The  $x_1$  displacement cannot be measured and, therefore,  $k_1$  and  $k_4$  stiffnesses should be joined with  $k_2$  and  $k_5$  stiffnesses.

$$\begin{aligned}
 -M_R \cdot \omega^2 \cdot x_1 + k_2 (x_2 - x_3) + k_5 (x_4 - x_5) + C \cdot j\omega \cdot x_1 &= F(\omega) \\
 x_1 &= (l_1 \cdot x_2 + l_2 \cdot x_4) / (l_1 + l_2) \\
 k_2 (x_2 - x_3) \cdot l_1 &= k_5 (x_4 - x_5) \cdot l_2 \\
 -M_U \cdot \omega^2 \cdot x_3 - k_2 (x_2 - x_3) + k_3 x_3 &= 0 \\
 -M_L \cdot \omega^2 \cdot x_5 - k_5 (x_4 - x_5) + k_6 x_5 &= 0
 \end{aligned}$$

**Eq. 2 Equations of motion simplified for the case when no air gap sensors are present.**

<sup>3</sup> Rotor vibrating mass is, practically, the same as the real rotor mass; For  $M_U$  and  $M_L$ , this is not true and must be determined based on vibration measurements

The  $x_1$  displacement is determined from the measured  $x_2$  and  $x_4$  displacements with the assumption that the rotor is moving between positions 2 and 4 as a solid (rigid) body. In the simplified model, there are 7 unknown values to be identified and 6 different relations being defined from the measurement results. To make the system consistent one parameter must be taken from the construction documentation. This will be the rotor generator mass since the real mass is equal to the vibrating mass which is not the case for the bracket and stator masses. These masses must be determined by measuring the vibrational response.

Since the measurements were performed in during run-up (or run-down) regime, the force is pure mechanical unbalance force of the form  $F(\omega) = F_0 \cdot \omega^2 \cdot \sin(\omega t)$

### VIBRATION-RELATED PARAMETERS IDENTIFICATION BASED ON THE SIMPLIFIED MODEL

As a first step, identification is performed based on the simplified model since, when the unit started operation, no air gap sensors were installed. If the equation system (Eq. 2) is normalized with rotor mass  $M_R=1$  there are 6 variables necessary for the identification. Since there are 6 equations, the system is completely determined and the stiffnesses  $k_2$ ,  $k_3$ ,  $k_4$  and  $k_5$  with vibrating masses  $M_U$  and  $M_L$  will be determined from experimentally obtained equations. All of the stiffnesses and masses are also normalized to  $M_R = 1$  which means that the numerical values for the stiffnesses and masses are obtained by multiplication of the identified values with the real rotor mass.

For the case study in question, the rotor mass is  $M_R = 210\,000$  kg.

From the 1x harmonic trends, the transfer functions for relative and absolute vibrations are defined which are measured directly by the installed vibration sensors. From the last two relation in Eq. 2, the transfer functions are obtained:

$$\begin{aligned} (x_2-x_3)/x_3 &= x_{rel, UGB}/x_{abs, UGB} = k_3/k_2 - (M_U/k_2) \cdot \omega^2 \\ (x_4-x_5)/x_5 &= x_{rel, LGB}/x_{abs, LGB} = k_6/k_5 - (M_L/k_5) \cdot \omega^2 \end{aligned}$$

*Eq. 3 Transfer functions for a model.*

On the left side of the Eq. 3 there is a ratio of the relative and absolute vibrations of UGB and LGB which are the functions of frequency. Since the relative and absolute vibrations are in phase, the ratio of vibration vectors comes down to the ratio of relative and absolute vibration vector modulus.

For each of the transfer functions it is necessary to take data (from measurements shown on Fig. 1) on 2 different frequencies so the 4 relations between vibration-related parameters  $k_2$ ,  $k_3$ ,  $k_4$ ,  $k_5$ ,  $M_L$  and  $M_U$  can be obtained.

From the first equation in Eq. 2 another relation between the system variables is obtained

$$\begin{aligned} -M_R (\omega_{KR})^2 x_1(\omega_{KR}) + k_2 \cdot [x_2(\omega_{KR}) - x_3(\omega_{KR})] + k_5 \cdot [x_4(\omega_{KR}) - x_5(\omega_{KR})] &= 0 \\ x_1 &= (l_1 \cdot x_2 + l_2 \cdot x_4) / (l_1 + l_2) \\ k_2 \cdot (x_2 - x_3) \cdot l_1 &= k_5 \cdot (x_4 - x_5) \cdot l_2 \end{aligned}$$

*Eq. 4*

If the critical speed is known (from Fig. 1 it's visible that the  $n_{crit} = 540$  rpm) – the fact that at the critical speed the elastic and inertial forces are in balance can be used and also that the external force is balanced by the damping force. This is true only for critical speed.

With this relation and with the condition that the torque forces within the bearing relative to the center of mass are equal to zero, 6 equations to determine stiffnesses and masses are obtained. All of the conditions to satisfy these 6 equations are obtained from measurements.

The calculated stiffnesses and vibrating masses with rotor mass  $M_R = 210\,000$  kg, taken from the documentation are:

- $k_2 = 447$  kN/mm (UGB stiffness)
- $k_3 = 2814$  kN/mm (upper bracket stiffness)
- $k_5 = 321$  kN/mm (LGB stiffness)
- $k_6 = 8350$  kN/mm (lower bracket stiffness)
- $M_U = 168.000$  kg (upper bracket + generator stator masses)
- $M_L = 19000$  kg (lower bracket mass)

When the unit operates, the bearing stiffnesses change significantly. This is dependent on the thrust collar thermal dilatations on UGB and LGB and the reduction of bearing clearances during temperature increase. This is especially true on LGB which is a combined guide and thrust bearing.

In order to monitor the bearing clearances on both generator guide bearings, one year in operation – 4 sensors were installed on each bearing symmetrically in the bearing segments plane.

On Fig. 3 trends of UGB and LGB bearing clearances are shown and the amplitude of 1x relative and absolute vibration harmonics in the generator regime from the cold start and UGB and LGB segment temperatures.

On both bearings significant differences in the transfer function amplitudes between relative and absolute vibrations are noted. During the bearing segment temperature increase, the bearing clearances reduce rapidly and, accordingly, the oil film stiffnesses increase. From the relation of relative vibrations in cold start and after 2 hours one can simply calculate that the UGB stiffness ( $k_2$ ) has increased 1.85 times and LGB ( $k_5$ ) 2.72 times.

So, when the unit is hot, the UGB and LGB stiffnesses are:

- $k_2^* = 827 \text{ kN/mm}$
- $k_3^* = 837 \text{ kN/mm}$

The other vibration-related parameters remain the same.

From these data, one can simply calculate that the unit critical speed when the unit is hot will increase from 540 rpm to ~800 rpm.

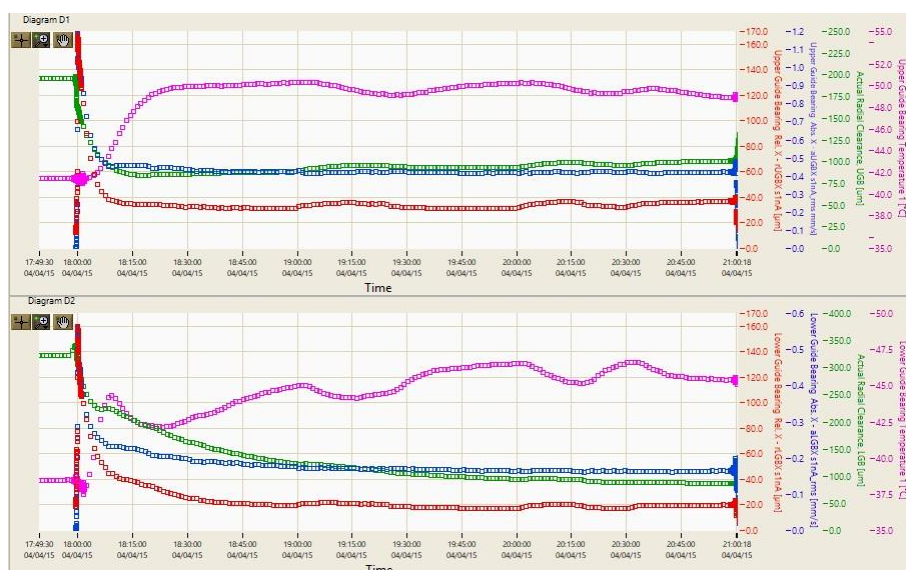


**Fig. 3 UPPER DIAGRAM: UGB – relative vibrations – direction X (red), UGB – absolute vibrations – direction X (blue), UGB – actual radial clearance (green), UGB – guide bearing temperature (purple). LOWER DIAGRAM: LGB – relative vibrations – direction X (red), LGB – absolute vibrations – direction X (blue), LGB – actual radial clearance (green), LGB – guide bearing temperature (purple).**

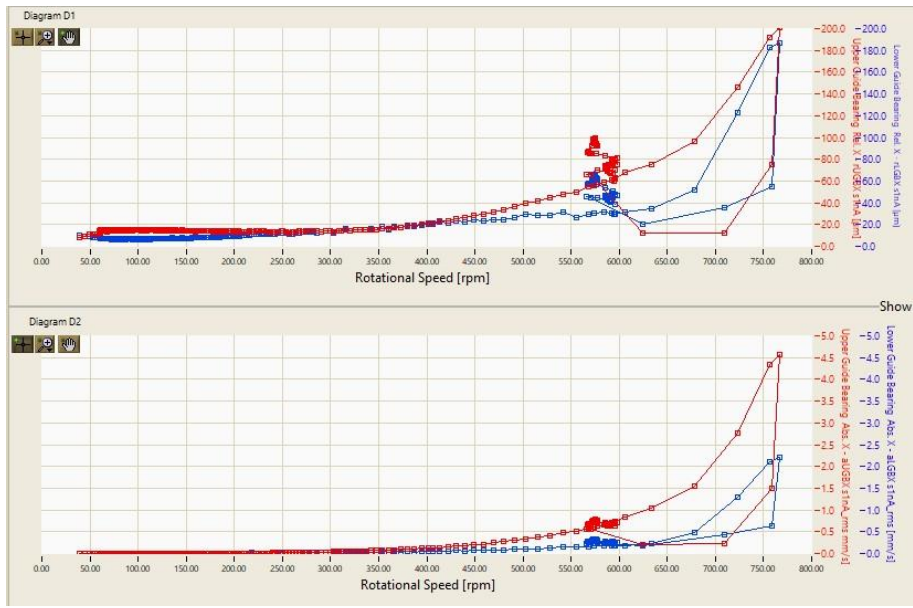


**Fig. 4 UPPER: UGB – relative vibrations (μm)– direction X (red), LGB – relative vibrations (μm)– direction X (blue). LOWER: UGB absolute vibration (mm/s)- direction X (red), LGB absolute vibrations (mm/s)- direction Y (blue) in load rejection test from 160 MW.**

The critical speed for hot bearings can be identified from the 1x harmonic relative and absolute vibrations trends when the unit slowly accelerates (or freely runs-down after load rejection). Fig. 4 shows the trends of relative and absolute vibrations after 160 MW load rejection. The unit reaches the maximum rotational speed (which is 760 rpm for 160 MW load rejection) very fast (after a couple of seconds) and then freely runs down with no brakes being applied.

At rotational speed above 600 rpm, a resonant effect is seen, that is – increase in vibrations becomes significantly faster than the forces due to mass unbalance which is the only force acting in a free run-down, when the electromagnetic forces are not-present and the water intake in the turbine is closed.

By extrapolating the vibrational trends – critical speed of  $n_{crit} = 802$  rpm is obtained which is almost identical to the calculations based on the bearing stiffnesses in hot state. The extrapolation procedure is conducted based on the assumption that the system (and its vibrational response) near the critical speed behaves like a simple vibrational system with one degree of freedom. With this assumption, the extrapolated part of the resonance curve depends only on critical speed position and damping.

The calculation procedure is shown in Fig. 5. From vibration response shown on Fig. 4 three points on different rotational speeds should be chosen. Blue curve shows relation between possible critical speed and damping factor  $\xi$  ( $\xi = C/C_{crit} = C/2 \cdot \omega_{crit}$ ) if two of three points are on vibration response curve. Black curve is the same for another two of three points. Common point (red point on fig 5) define critical speed and damping factor for the case where all three points are on the same resonant curve.

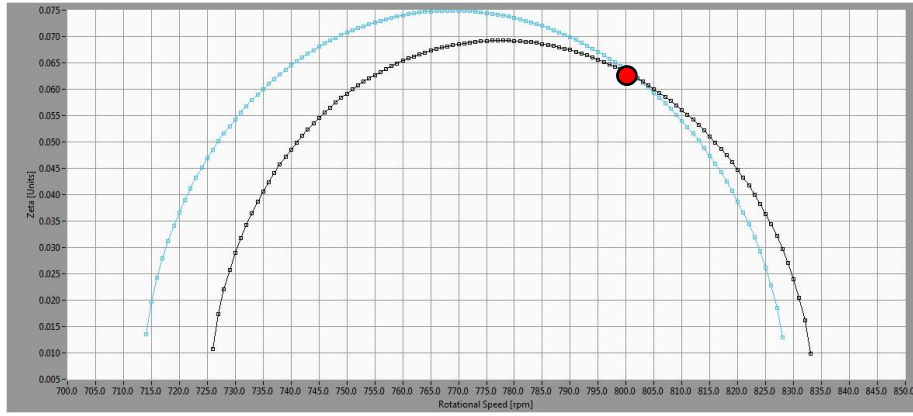


**Fig. 5 Critical speed determination. The red point indicates where the critical speed is calculated from response shown in Fig. 4,  $n_{crit} = 802$  rpm,  $C/C_{crit} = \xi = 0.06$ .**

Result of this procedure is  $n_{crit} = 802$  rpm, and  $\xi = C/C_{crit} = 0.06$ .

For this unit, the identification procedure for a cold unit is simplified by the fact that it could be directly measured. For most units this is not the case. When the first critical speed is outside the rotational speed which the unit can achieve, it is necessary to extrapolate the measurement results and obtain the critical speed as accurately as possible.

Already these results with a simplified model show that there is a large discrepancy between the critical speed obtained experimentally (about 802 rpm) and the designed value (1150 rpm).

### VIBRATION-RELATED PARAMETERS IDENTIFICATION BASED ON THE COMPLEX MODEL

After one year of operation, air gap sensors were installed onto the stator inside the generator air gap. These sensors enable the identification of the shaft stiffness between the rotor rim and bearings.

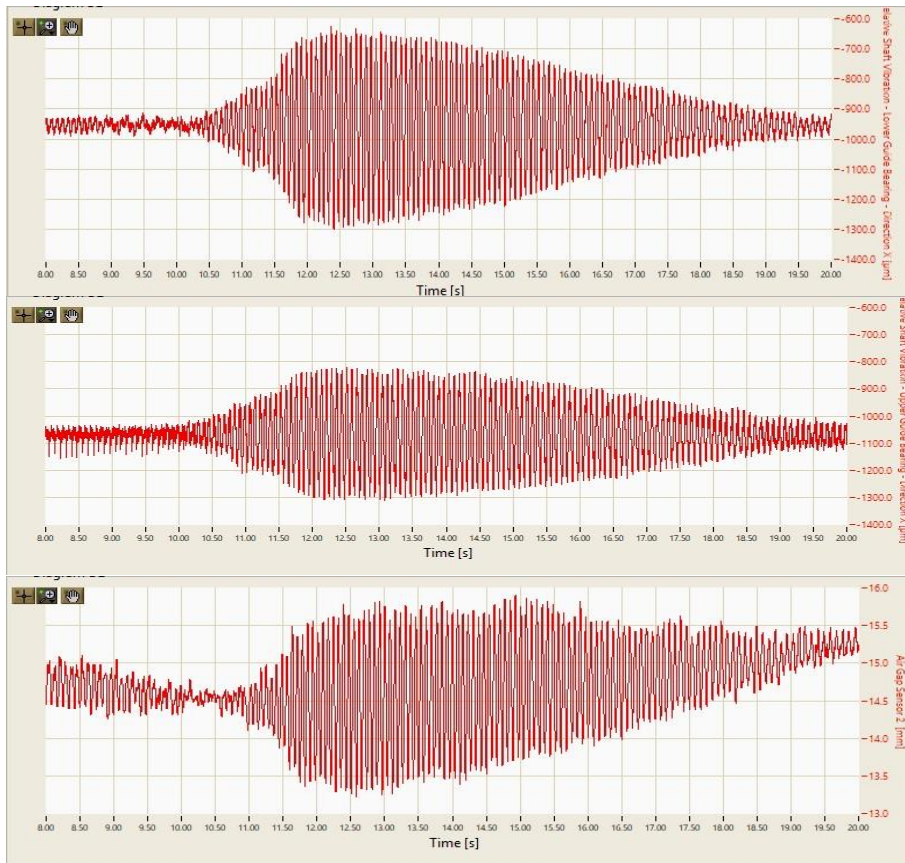
Table 1 shows the maximum amplitudes of vibrational displacements on the 1x harmonic on all 5 positions for 75%, 85% and 100% load rejections. The  $x_2$  and  $x_4$  displacements are calculated from the measured positions and all other are determined from vibrations recorded at load rejection tests.

Absolute rotor vibr. (peak to peak) [ $\mu\text{m}$ ]	75% load rejection	85% load rejection	100% load rejection
$x_1$	450	810	2200
$x_2 - x_3$	140	250	440
$x_4 - x_5$	120	250	620
$x_3$	59	90	240
$x_5$	30	61	170
$x_2$	199	340	680
$x_4$	155	311	790
max rpm	<b>736</b>	<b>750</b>	<b>790</b>

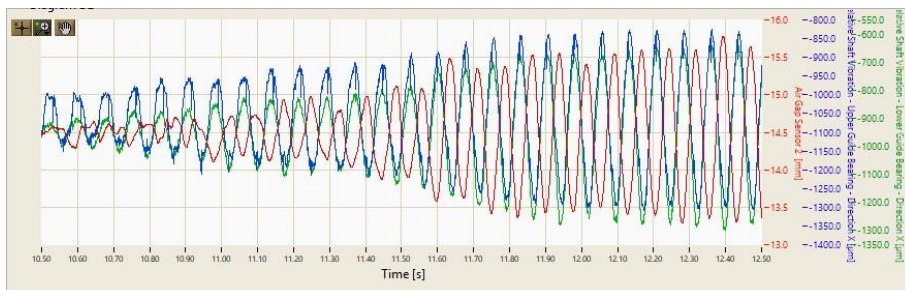
Table 1. Maximum vibration amplitudes and rotation speed in load rejection tests

Fig. 6 shows the waveforms of UGB and LGB relative vibrations ( $x_2-x_3$  and  $x_4-x_5$  displacements) and the air gap signal from which only the rotor displacement on rotational frequency has been extracted. This is, according to Table 1, displacement  $x_1$ .

Fig. 7 shows the same waveforms in a shorter time-span. Air gap sensor is installed at the opposite side of the vibration sensor and, therefore, the air gap signal is out-of-phase with the vibration signals and the vibrations in the air gap and bearings are in-phase.



**Fig. 6 UPPER DIAGRAM: Relative shaft vibrations on LGB. MIDDLE DIAGRAM: Relative shaft vibrations on UGB. LOWER DIAGRAM: Rotor rim vibrations. All during load rejection test from 180 MW.**



**Fig. 7 Red: Rotor rim vibrations, blue: UGB relative shaft vibrations, green: LGB relative shaft vibrations. At the beginning of load rejection test from 180 MW.**

The rotor-rim vibration amplitude (which is a change in air gap at rotational frequency) is multiple times larger than are the shaft vibrations in the UGB and LGB planes. This is a sure sign that the shaft between the rotor rim and the bearings are getting deformed. From the vibration amplitude relationship – the shaft between the rotor rim, the bearings and the oil film stiffnesses can be determined.

The stiffnesses  $k_2^*$  and  $k_5^*$  determined in the previous analysis procedure are, basically, a serial connection of all the stiffnesses between the upper (and lower) bracket and rotor rim.

The relation of vibrational displacements in Table 1 show that the oil film stiffness, when the bearings are hot and when the vibrational displacements are large, are at least two times higher then the shaft stiffness. At the rotor position in the LGB direction at 100% load rejection (when the vibrational displacements are the largest) this relation goes up to 3.5 times.

For  $k_1$  and  $k_4$  stiffnesses calculations and also oil film stiffness of hot bearings ( $k_2$  and  $k_5$ ) from experimentally obtained  $k_2^*$  and  $k_5^*$  one uses the most undesirable situation (100% load rejection) one obtains:

- $k_1 = 1060 \text{ kN/mm}$  (shaft stiffness between rotor-rim and UGB)

- $k_4 = 1200$  kN/mm (shaft stiffness between rotor-rim and LGB)
- $k_2 = 3720$  kN/mm (oil film stiffness for a hot UGB)
- $k_5 = 2760$  kN/mm (oil film stiffness for a hot LGB)

For a cold unit – the  $k_1$  and  $k_4$  stiffnesses remain the same and the UGB and LGB oil film stiffnesses are determined from  $k_2$  and  $k_5$  for a simplified model in cold state (which are 447 kN/mm and 321 kN/mm). So, for cold bearings one obtains:

- $k_1 = 1060$  kN/mm (shaft stiffness between rotor-rim and UGB)
- $k_4 = 1200$  kN/mm (shaft stiffness between rotor-rim and LGB)
- $k_2 = 800$  kN/mm (oil film stiffness for a cold UGB)
- $k_5 = 440$  kN/mm (oil film stiffness for a cold LGB)

By comparing the stiffnesses for cold and hot bearings it becomes clear that the unit's vibrational properties are so different they can be hardly compared. In cold state, the critical speed ( $n_{crit} = 540$  rpm) is dominantly dependant on the oil film stiffnesses and in the hot state ( $n_{crit} = 802$  rpm) on the shaft stiffnesses.

With regards to the non-linear properties of the oil film, which is manifested in oil film stiffness dependency on the bearing clearance, any rotational speed between 540 and 810 rpm is, potentially, a critical speed for this unit. If the unit suffers load rejection and the rotational speed increases, the vibrational response will depend on the bearing clearance at that moment.

For the unit's vibrational stability, the dynamics in hot state is much more important because the load rejections rarely occur immediately after the run-up when the bearings are still cold.

But the dynamical state of this unit in a hot state is, practically, not very dependent on the bearing stiffnesses. If the temperature of the bearings would increase which would, consequently, reduce their clearance even further the critical speed would remain the same. This is because the total rotor and bearing stiffness is defined by shaft stiffness.

Now that all of the dynamical unit parameters have been determined one can form a simulation model. The model is based solely on experimentally determined stiffnesses and vibrating masses.

### **SIMULATION OF THE VIBRATIONAL STATE DISTURBANCE BASED ON THE EXPERIMENTALLY IDENTIFIED SIMULATION MODEL**

The simulation model is realized on the LabVIEW programming platform (the same platform on which the measurements were performed) so that, for the input parameters, it can use directly stored vibration responses at the described positions.

As an external force the function shown represents the unbalance force as the only force on the unit rotor in mechanical rotation without excitation.

Fig. 8 and Fig. 9 show calculated responses for the stiffnesses and vibrating masses in a cold and hot state. The first critical speed completely matches that determined experimentally which is the expected result since the model contains only experimentally determined vibration parameters. The simulation model is linear which is why the calculated vibrational responses have symmetrical slopes with regards to the first critical speed position (unlike the diagrams on Fig. 1 which have different slopes). The first step to further improve the simulation model is to introduce the non-linear characteristics of the oil film stiffness.

The simulation model shows the existence of the second critical speed at 1320 rpm in cold condition, and 1450 in hot condition. Based on the model, one more critical speed (the model takes into account the existence of three concentrated masses whose values are obtained experimentally) which is above 1600 rpm and isn't shown in the simulation diagrams.

On the first critical speed the rotor ( $M_R$ ) and stator with upper bracket ( $M_U$ ) vibrate in-phase. On the second critical speed (1320 rpm) the rotor and stator vibrate out-of-phase. In the normal unit operation this speed is not achievable. The highest achievable speed is 790 rpm and occurs after 180 MW load rejection. The runaway speed is 910 rpm.

Fig. 10 shows the simulation results when the masses  $M_U$  and  $M_L$  are neglected ( $M_U = M_L = 0$ ). The critical speed, for the same stiffness parameters, has increased from 790 to 830 rpm. The second critical speed is non-existent in this model because it was assumed that the stator vibrating mass is equal to zero.

These are, practically, the conditions for rotor critical speed calculations being performed by the generator producers. The calculations are performed with finite element method. The rotor is modeled with finite elements and the influence of the non-rotational parts of the aggregate is being taken into account only through bearing stiffnesses as the calculation boundary condition.

The simulation results, shown on show that such an approach is insufficient and the results are larger critical speeds than present on the unit in reality. If the stator mass is neglected (in the case study presented, the stator is 80% of the rotor mass) the critical speed obtained is by 40 rpm higher than the one that is experimentally obtained (830 rpm vs. 790 rpm).

The described results show, without a doubt, that to calculate hydro-unit critical speed correctly one should perform the calculations for the entire construction instead of just the unit's rotor.

Simulation model, completely designed from measuring procedure, can be very succesfully used for cakculating vibrational response for different fauts (reducing bearing stiffnes, foundation cracks, axle cracks etc. changing unbalance etc.)

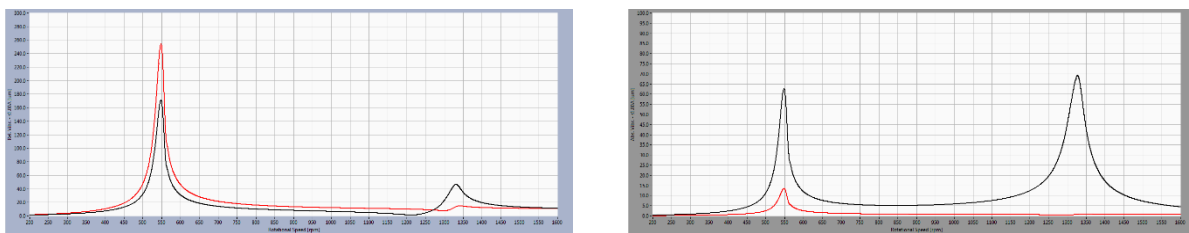


**Fig. 8** Calculated vibration response for cold condition, UGB-black, LGB-red. LEFT: Relative vibrations, RIGHT: Absolute vibrations

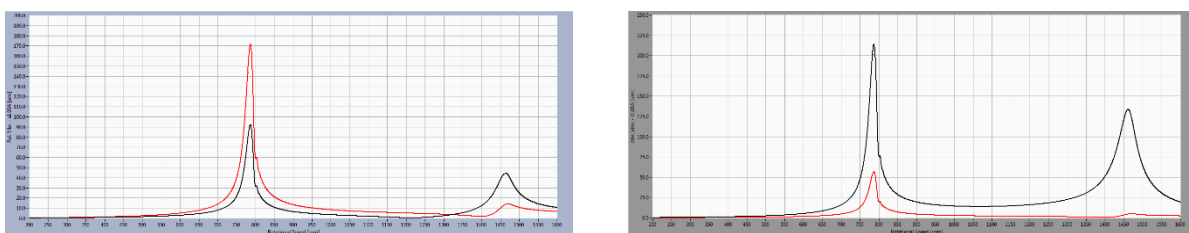


**Fig. 9** Calculated vibration response for hot condition, UGB-black, LGB-red. LEFT: Relative vibrations, RIGHT: Absolute vibrations

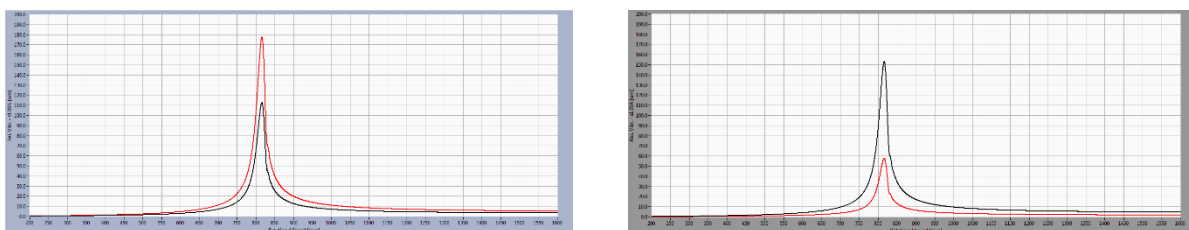


**Fig. 10** Calculated vibration response for hot condition with no stator and bracket masses, UGB-black, LGB-red LEFT: Relative vibrations, RIGHT: Absolute vibrations

## CONCLUSION

Big differences between real dynamical parameters (stiffnesses, critical speed etc.) and parametres calculated in hydro-unit design procedure that are mostly present in practise, cause very often unexpected measuring results in vibration measuring and analysis procedure.

That is the main reason for defining experimental identification procedure, based only on vibration measuring results, for defining the real values of bearing stiffnesses, foundation structure stiffnesses, generator stator and bracket stiffnesses, rotor, stator and bracket vibrating masses and real critical speed.

As an example for experimental identification procedure vibration analysis results on a 180 MW revisable hydro-unit are used. Identification procedure shows that there is a very big changing of bearing clearance of UGB and LGB is present during heating of unit. The result of bearing clearance changing is a big

changing of UGB and LGB stiffness and increasing critical speed from 540 rpm in cold conditions to 802 rpm in hot conditions.

After all necessary vibration parameters are identified a simulation model can be established. Simulated vibration response for rotational speed 0 - 800 rpm should be very similar to the measured response because in model only experimentally identified vibration parameters are introduced. Using this model one can simulate vibration response in case that some faults (as reducing bearing stiffness, foundation cracks, axle cracks etc.) in hydro-unit structure are present.

For experimental identification hydro-unit must be equipped with all necessary vibration sensors and air gap sensors.

## REFERENCES

- [1] Mechanical vibration – Evaluation of machine vibration by measurements on non-rotating parts – Part 5: Machine sets in hydraulic power generating and pumping plants, ISO 10816-5, 2000.
- [2] Mechanical vibration – Evaluation of machine vibration by measurements on rotating shafts – Part 5: Machine sets in hydraulic power generating and pumping plants, ISO 7919-5, 2005.
- [3] Mechanical vibration -- Measurement and evaluation of machine vibration -- Part 1: General guidelines, ISO 20816-1, 2016.
- [4] J. P. Den Hartog, Mechanical Vibrations, McGraw Hill, 1956
- [5] C. M. Harris, A. G. Piersol: Harris shock and vibration handbook, McGraw Hill, 2002
- [6] Specific technical requirements for hydro generators, IEC 60034-32/WD Edition 4.0, 2018

## AUTHOR BIOGRAPHIES

### **Ozren Husnjak (Veski Ltd, Croatia):**

Master of Science, Department of Physics, Faculty of Science in Zagreb.

Four years (2002.- 2006.) employed as an assistant at Department of Physics.

Last 11 years (2006.-) employed at Veski on software development, vibration troubleshooting and problem solving.

Ozren worked on numerous MCM projects as system commissioning engineer and as a technical expert for machine condition evaluation.

### **Ozren Oreskovic (Veski Ltd, Croatia):**

Education: Master degree at Faculty of Mechanical Engineering and Naval Architecture in Zagreb

Working experience: over 11 years of experience, employed at Veski.

From 2004-2009 Worked as Field Service Engineer commissioning MCM systems and troubleshooting vibration problems.

From 2009-2012– Working as Sales and Marketing manager at Veski

From 2012 – Works as Managing director at Veski

### **John Letal (Iris Power, Canada):**

John Letal is a Rotating Machines Engineer at Iris Power responsible for supporting mechanical monitoring initiatives. Prior to Iris, he spent 7 years with Siemens TurboCare in field service troubleshooting large rotating equipment using vibration analysis. John holds a Master's degree in Mechanical Engineering from the University of Toronto and is registered as a Professional Engineer in Canada.

**Fabian Kaica (Fabian Kaica Consulting, Australia):**

Fabian Kaica is a professional mechanical engineer with 35 years international experience in Hydro Power Engineering based in Australia. Fabian has specialised in: Asset Management, Reliability Improvement including Root Cause Analysis and Failure Mode identification, Condition Monitoring, Vibration Diagnostics.

Since 2012 Fabian has worked as an independent Specialist Hydro Mechanical Engineer.